A critical analysis of chemical and electrochemical oxidation mechanisms in Li-ion batteries

Evan Walter Clark Spotte-Smith,[†,‡,#] Sudarshan Vijay,[†,¶,#] Thea Bee Petrocelli,[†] Bernardine L. D. Rinkel,[§,‖] Bryan D. McCloskey,[§,‖] and Kristin A. Persson[*,†,⊥]

†*Department of Materials Science and Engineering, University of California – Berkeley, 210 Hearst Memorial Mining Building, Berkeley, CA, 94720 USA*

‡*Materials Science Division, Lawrence Berkeley National Laboratory, 1 Cyclotron Road, Berkeley, CA, 94720 USA*

¶*Present address: VASP Software GmbH, Sensengasse 8, A-1090 Vienna, Austria*

§*Department of Chemical and Biomolecular Engineering, University of California – Berkeley, 201 Gilman Hall, Berkeley, CA, 94720 USA*

‖*Energy Storage and Distributed Resources, Lawrence Berkeley National Laboratory, 1 Cyclotron Road, Berkeley, CA, 94720 USA*

⊥*Molecular Foundry, Lawrence Berkeley National Laboratory, 1 Cyclotron Road, Berkeley, CA, 94720 USA*

#*These authors contributed equally to this work*

E-mail: kapersson@lbl.gov

https://doi.org/10.26434/chemrxiv-2023-qr36w **ORCID:** https://orcid.org/0000-0003-1554-197X Content not peer-reviewed by ChemRxiv. **License:** CC BY-NC 4.0

Abstract

Electrolyte decomposition in lithium-ion batteries (LIBs) remains a challenge, limiting the lifetime of commercial cells and slowing the adoption of next-generation energy storage technologies. Fundamental mechanistic understanding of electrolyte degradation is critical to enable the design of next-generation LIB technologies. To date, most explanations for electrolyte decomposition at LIB positive electrodes rely on either electrochemical oxidation of ethylene carbonate (EC) or chemical oxidation of EC by evolved singlet oxygen ($^1O_2$). In this work, we discuss the feasibility of these mechanisms based on density functional theory calculations. We find that electrochemical oxidation is thermodynamically unfavorable at any potential reached during normal LIB operation, while elementary reaction mechanism analysis suggests that previously reported reactions between EC and $^1O_2$ are kinetically limited at room temperature. Our calculations suggest an alternative mechanism, in which EC reacts with superoxide (O_2^{-1}) and/or peroxide (O_2^{-2}) anions. This work provides a new perspective on LIB electrolyte decomposition and motivates further experimental and computational studies to fully understand reactivity at positive electrodes.

Introduction

Electrolyte design is one of the most significant remaining challenges in the development of lithium-ion battery (LIB) technologies. To be practically useful, an electrolyte must simultaneously possess a number of key properties, including high Li^+ conductivity and transference number, low viscosity, and compatibility with the battery's positive and negative electrodes.[1] The latter requirement — that electrolytes must be stable at both electrodes — is especially challenging to meet. To achieve high energy density, LIBs operate at extreme potentials, as low as 0.1 V for common graphitic negative electrodes (in this work, all potentials are referenced to the reduction potential of Li^+) and, depending on the composition of the positive electrode, as high as 4.2–4.5 V for lithium nickel manganese cobalt oxides (NMC)[2] or

https://doi.org/10.26434/chemrxiv-2023-qr36w **ORCID:** https://orcid.org/0000-0003-1554-197X Content not peer-reviewed by ChemRxiv. **License:** CC BY-NC 4.0

4.5–4.8 V for novel disordered rock salts (DRX).[3] In the reactive environment created at these potentials, most electrolytes tend to degrade over time, leading to lowered Coulombic efficience and irreversible capacity loss.[4] To continue to improve the lifetime of LIBs and to enable the deployment of next-generation electrodes like DRX, it is essential to either prevent electrolyte decomposition reactions entirely or else to promote the formation of passivation films, known as solid-electrolyte interphases (SEIs) when formed on the negative electrode[5] and cathode electrolyte interphases (CEIs) when formed on the positive electrode.[6]

Commercial LIB electrolytes are solutions composed of lithium hexafluorophosphate ($LiPF_6$) dissolved in a mixture of organic carbonates such as ethylene carbonate (EC) and ethyl methyl carbonate.[7,8] For many years, SEI formation mechanisms for carbonate/$LiPF_6$ electrolytes at LIB negative electrodes have been studied in detail; experimentally observed products have been mapped to reactants through a combination of experimental characterization techniques,[9,10] atomistic modeling,[11–13] and chemical reaction network (CRN) analysis.[14,15] By comparison, degradation mechanisms at positive electrodes have received less attention and are less well understood.

Electrochemical and chemical oxidation have been proposed in the literature as explanations for EC decomposition at potentials $\gtrsim$ 4 V[16,17] (in general, exact onset potentials for electrolyte decomposition and other degradation processes depend on the electrode composition, among other factors).[18] In electrochemical oxidation, EC loses an electron to the electrode, after which it can react with other salt and solvent molecules.[19] Chemical oxidation does not involve direct electron transfer between the electrode and electrolyte but instead involves attack by so-called "reactive oxygen". Diatomic oxygen (O_2) has been detected evolving at high potentials from transition metal oxide positive electrodes, including NMC ($\sim$ 4.2 V)[20,21] and DRX ($\sim$ 4.5 V).[22,23] Some reports studying NMC materials claim that this O_2 is released in the singlet excited state ($^1O_2$),[10,24–27] which is considered to be more reactive than the triplet ground state ($^3O_2$).[28,29]

In this work, we evaluate both these proposed reaction mechanisms using density func-

https://doi.org/10.26434/chemrxiv-2023-qr36w **ORCID:** https://orcid.org/0000-0003-1554-197X Content not peer-reviewed by ChemRxiv. **License:** CC BY-NC 4.0

tional theory (DFT) calculations. We show that electrochemical oxidation of EC is unlikely to occur at typical operating voltages in LIBs and that chemical oxidation by singlet oxygen is potentially also infeasible due to sluggish kinetics. These findings suggest that the potential-dependent degradation of EC at LIB positive electrodes occurs via alternate mechanisms. We conclude by hypothesizing a decomposition route that requires neither electrochemical oxidation nor reactions with $^1O_2$. Specifically, based on observations of partial oxygen redox to peroxide ($O_2{}^{-2}$) or "peroxo-like" species in transition metal oxide electrodes and reports of reactions between organic carbonates and superoxide anions ($O_2{}^{-1}$), we suggest that oxygen anions may favorably react with and degrade EC.

Electrochemical oxidation

In this section, we discuss the feasibility of EC decomposition through electrochemical oxidation. The hypothesis that EC reacting electrochemically at battery positive electrodes is suspect based on the available experimental literature. Reported oxidation potentials for EC vary, but if we limit our consideration to measurements made using non-reactive electrodes such as platinum or glassy carbon — aiming to eliminate the possibility of reactions between EC and the electrode surface — the reported values are between 4.8 V and 6.5 V.[16,30–34] Even the low end of this range is considerably higher than typical LIB operating potentials. However, Chen[35] recently suggested that concentration effects may lower the effective oxidation potential of EC. That is, if the products of electrochemical oxidation are sufficiently short-lived or in sufficiently low concentration at steady-state, the reaction could become favorable at potentials below EC's standard oxidation potential.

To evaluate the possibility of electrochemical EC oxidation, we consider the elementary steps of charge transfer to EC. In the simplest mechanism, EC is oxidized as,

$$\mathrm{EC} \longrightarrow \mathrm{EC}^+ + \mathrm{e}^-, \tag{1}$$

https://doi.org/10.26434/chemrxiv-2023-qr36w **ORCID:** https://orcid.org/0000-0003-1554-197X Content not peer-reviewed by ChemRxiv. **License:** CC BY-NC 4.0

where the e^- is an electron and EC^+ is the oxidized form of EC (see Figure 1a). Our computations (see Supporting Information for computational methods) show that this reaction has a standard oxidation potential of $E^0 = 6.98$ V, which is significantly higher than the experimentally measured range.

The mechanism of EC oxidation may change when additional solvent molecules are involved. Xing and Borodin[19] previously applied DFT and Møller-Plesset perturbation theory to study the oxidation of a cluster of two EC molecules, EC_2. They found that, during the optimization of the oxidized cluster $EC_2{}^+$, a proton transferred from one EC to the other, making the reaction overall,

$$2\,\mathrm{EC} \longrightarrow (\mathrm{EC{+}H})^+ + (\mathrm{EC{-}H}) + \mathrm{e}^-. \tag{2}$$

This spontaneous transfer of a proton implies that the initial elementary step of electrochemical EC oxidation is a concerted reaction involving both charge transfer and proton transfer. We confirm that, during DFT optimization of $EC_2{}^+$, proton transfer occurs, though this does not necessarily imply that EC oxidation is concerted. The calculated standard oxidation potential for this reaction is $E^0 = 5.80$ V using the free energies of the reactant and product clusters (Figure 1b, top), and $E^0 = 5.84$ V using reactants and products at infinite separation (Figure 1b, bottom), within the experimentally measured range at non-reactive electrodes.

Especially in the condensed phase, it can be difficult to determine if electron transfer reactions are stepwise (with charge transfer followed by additional bond cleavage and formation steps) or concerted.[36] Even if intermediates form following charge transfer in a stepwise mechanism, those intermediates may be too short-lived or in too small concentration to be experimentally observed. Although the calculated standard oxidation potential of the concerted dissociative oxidation given by Reaction 2 is in better agreement with experimental characterization, we cannot presently say with certainty if electrochemical EC oxidation follows a stepwise or concerted pathway. This is especially true given Chen's argument on

https://doi.org/10.26434/chemrxiv-2023-qr36w **ORCID:** https://orcid.org/0000-0003-1554-197X Content not peer-reviewed by ChemRxiv. **License:** CC BY-NC 4.0

concentration effects. Given this uncertainty, we must consider both stepwise and concerted dissociative electrochemical EC oxidation.

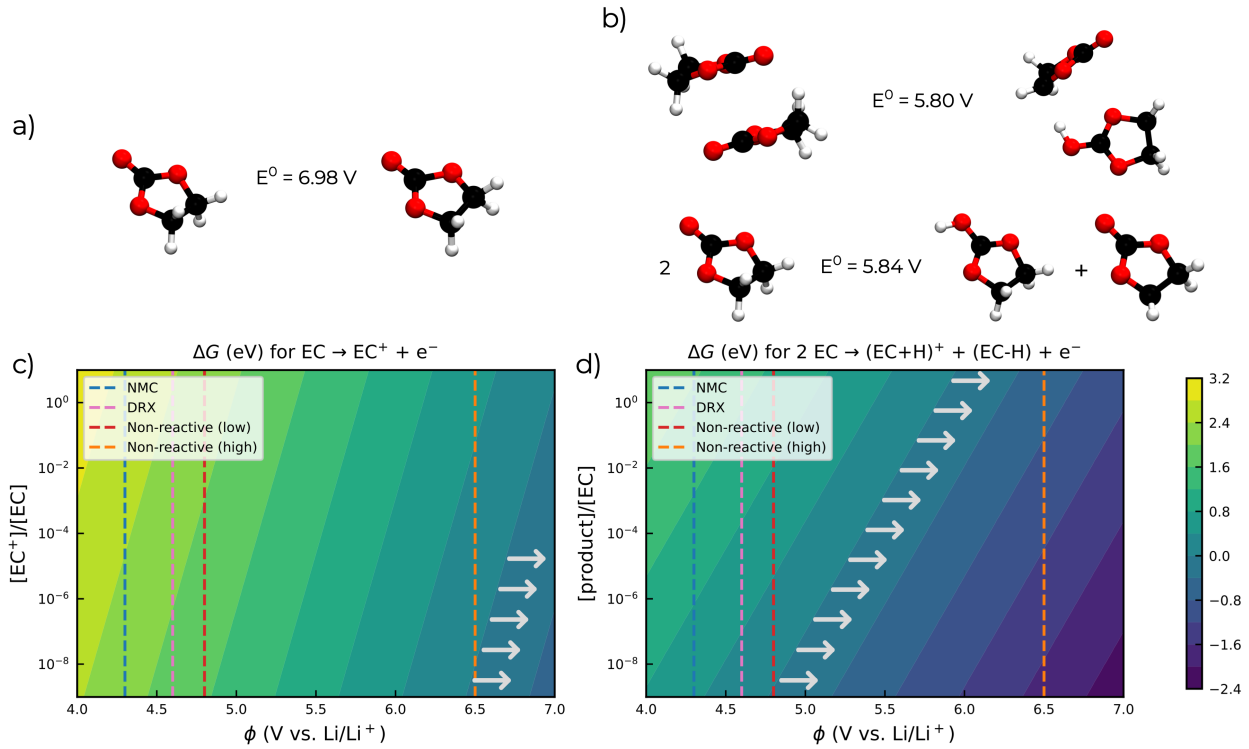

Figure 1: a) Depiction of the oxidation reaction EC $\longrightarrow$ $EC^+ + e^-$, with 3D structures for EC and EC^+. b) Depictions of the concerted dissociative oxidation reaction $2\,EC \longrightarrow (EC{+}H)^+ + (EC{-}H) + e^-$, with 3D structures of the reactants and products as clusters (top) and isolated molecules (bottom). c) (color scale) Free energy change, ΔG, for the electrochemical oxidation of EC, as a function of potential and relative concentration. d) ΔG for the concerted dissociative oxidation of EC as a function of potential and relative concentration, where we assume that $(EC{+}H)^+$ and $EC{-}H$ have the same concentration, denoted as [product]. Vertical lines in c) and d) indicate typical maximum potentials for example NMC (blue, shown at 4.3 V) and DRX (pink, shown at 4.6 V) positive electrodes, as well as the range of reported electrochemical oxidation potentials of EC at non-reactive electrodes (red and orange). For all points to the right of the arrow tails (at the $\Delta G = 0.0$ eV line), electrochemical EC oxidation is predicted to be thermodynamically accessible.

To determine whether electrochemical oxidation is feasible under battery operating conditions, we compute the free energy change (ΔG) as

$$\Delta G = \Delta G^0 + RT\ln(Q) - F\Delta\phi, \tag{3}$$

https://doi.org/10.26434/chemrxiv-2023-qr36w **ORCID:** https://orcid.org/0000-0003-1554-197X Content not peer-reviewed by ChemRxiv. **License:** CC BY-NC 4.0

where ΔG^0 is the free energy change under standard temperature, pressure, and concentration conditions at a fixed standard potential ϕ_0, R is the ideal gas constant, T is the absolute temperature in Kelvin, Q is the reaction quotient, which is,

$$Q = \frac{[\mathrm{EC}^+]}{[\mathrm{EC}]}, \tag{4}$$

for the stepwise oxidation given by Reaction 1 and,

$$Q = \frac{[\mathrm{EC{+}H}^+][\mathrm{EC{-}H}]}{[\mathrm{EC}]^2}, \tag{5}$$

for the concerted dissociative oxidation given by Reaction 2, F is Faraday's constant, and $\Delta\phi = \phi - \phi_0$ is the difference between the potential at the positive electrode and the reference potential. Here, we use the vacuum potential of the electron as ϕ_0.[37]

Neither the stepwise nor the concerted dissociative electrochemical oxidation reactions are feasible under standard conditions, with standard oxidation potentials significantly higher than 5 V. However, as indicated in Equation 3, the feasibility of Reactions 1 and 2 depend on both the operating potential ϕ and the relative steady-state concentrations of the oxidation products.

Figure 1 shows ΔG for different ϕ (x-axis) and relative concentrations (y-axis) for the stepwise (c) and concerted (d) mechanisms. The lower the relative concentration, (along the y-axis for a fixed x-axis value), the greater the favorability of the reaction. Likewise, the reaction is more favorable as the potential is increased (along the x-axis for a fixed y-axis).

At all relative concentrations considered (as low as 10^{-9}), we predict that a potential > 6 V would need to be applied for Reaction 1 to be thermodynamically favorable. Even considering possible error in our DFT calculations, this strongly suggests that the stepwise electrochemical oxidation of EC is not the dominant mechanism of EC degradation at LIB positive electrodes during normal battery operation. Because Reaction 2 has a considerably lower standard oxidation potential than Reaction 1, the concerted dissociative oxidation

https://doi.org/10.26434/chemrxiv-2023-qr36w **ORCID:** https://orcid.org/0000-0003-1554-197X Content not peer-reviewed by ChemRxiv. **License:** CC BY-NC 4.0

is more favorable at all potentials considered. The effect of relative concentration is also more significant on Reaction 2, which involves two products (see Equation 5). As such, Figure 1d shows that it could be possible for concerted dissociative EC oxidation to occur at applied potentials as low as $\sim$ 4.8 V. If the concerted dissociative mechanism is possible in real LIB electrolytes and the steady-state product concentrations are extremely low, it may be possible for some electrochemical EC oxidation to occur at some high-voltage positive electrodes. However, even in this case, we predict that electrochemical oxidation cannot occur at lower potentials used with e.g. NMC electrodes.

Chemical oxidation by $^1O_2$ is kinetically limited at room temperature

As we have predicted that electrochemical oxidation of EC is unlikely to occur at applied potentials relevant to LIB operation, we now study the feasibility of chemical oxidation by $^1O_2$. We compute the free energies and free energy barriers for reaction mechanisms previously proposed in literature, all taken at room temperature (298.15 K).

We identified two elementary mechanisms for chemical reactions between $^1O_2$ and EC (Figure 2). In the first (orange) pathway, originally suggested by Jung et al.,[24] $^1O_2$ initially reacts with EC to form water and 1,3-dioxolane-2,4-dione, a diketone species. The second (yellow) pathway, proposed by Freiberg et al.,[38] results in the formation of H_2O_2 and vinylene carbonate (VC).

The H_2O-forming pathway begins ($M_1 \longrightarrow M_2$; $\Delta G^{\ddagger} = 2.11$ eV) with $^1O_2$ abstracting a hydrogen atom and attaching to EC in a concerted reaction. The result of this attachment is a zwitterionic complex M_2. After a rotation ($M_2 \longrightarrow M_3$; $\Delta G = 0.10$ eV), a rearrangement occurs ($M_3 \longrightarrow M_4$; $\Delta G^{\ddagger} = 1.44$ eV), replacing the zwitterionic $-$OHO group with a hydroperoxide group ($-$OOH). We note that we considered a direct reaction between M_1 and M_4, but all attempts to locate a transition-state for $M_1 \longrightarrow M_4$ resulted in optimizing

https://doi.org/10.26434/chemrxiv-2023-qr36w ORCID: https://orcid.org/0000-0003-1554-197X Content not peer-reviewed by ChemRxiv. License: CC BY-NC 4.0

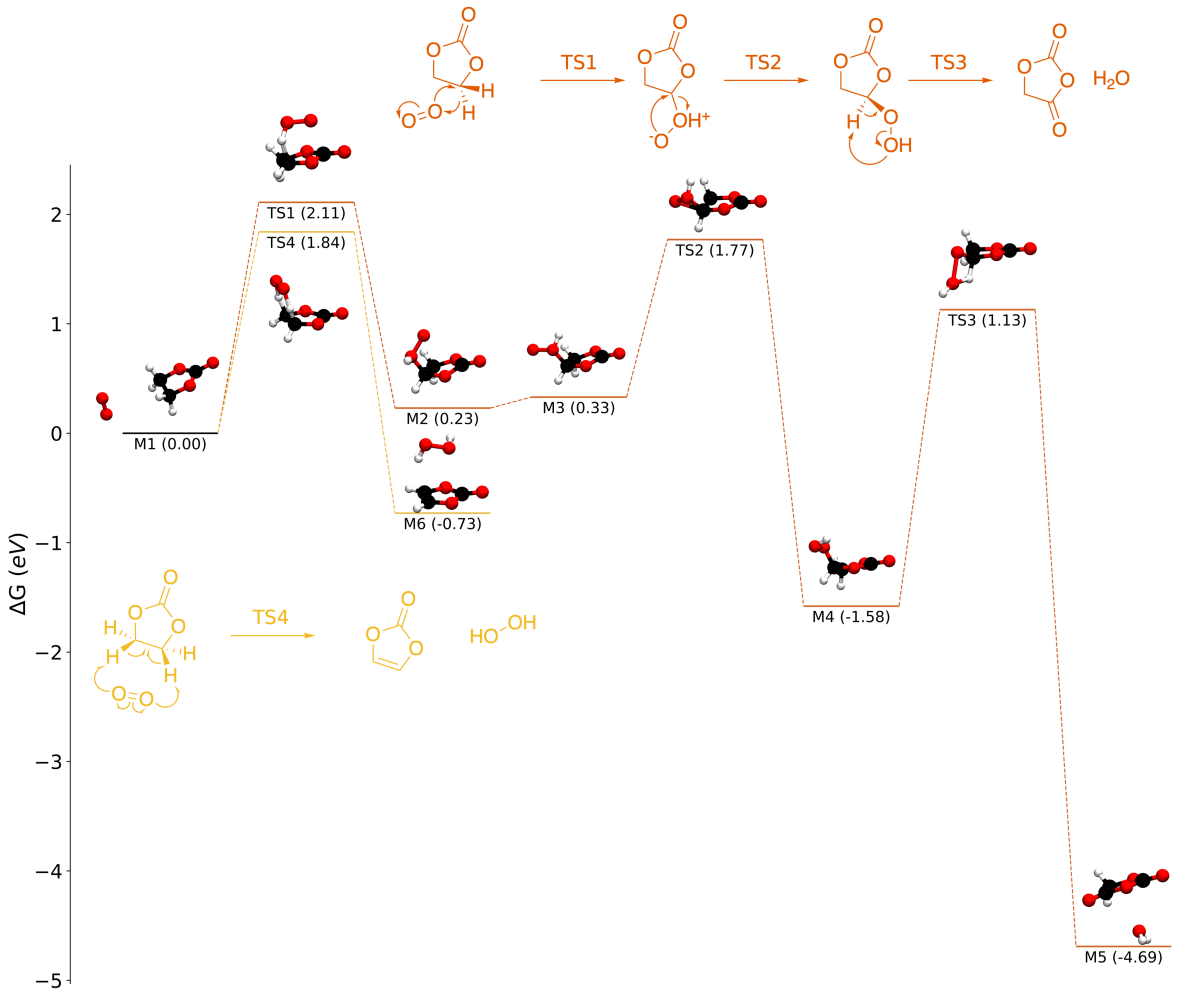

Figure 2: Energy diagrams for two reactions between $^1O_2$ and EC: one in which $^1O_2$ eventually forms H_2O and a diketone species (orange) and one in which $^1O_2$ abstracts two hydrogen atoms from EC to form H_2O_2 and vinylene carbonate (VC) in a single concerted step (yellow). Both pathways are thermodynamically favorable but severely kinetically limited.

either the $M_1 \longrightarrow M_2$ or the $M_3 \longrightarrow M_4$ transition-state. In the final step ($M_4 \longrightarrow M_5$; $\Delta G^{\ddagger} = 2.71$ eV), water is eliminated, leaving a ketone. While this pathway is overall thermodynamically favorable ($M_1 \longrightarrow M_5$; $\Delta G = -4.69$ eV), it is severely kinetically limited, with all three free energy barriers > 1.0 eV and two of three > 2.0 eV. To exemplify the sluggish kinetics, consider reaction $M_1 \longrightarrow M_2$ proceeding at room temperature in a pure EC solution (concentration ≈ 15 M) with a dissolved $^1O_2$ concentration of 1.56 mM (the solubility of O_2 in EC is discussed in the Supporting Information). Calculating the rate as,

https://doi.org/10.26434/chemrxiv-2023-qr36w **ORCID:** https://orcid.org/0000-0003-1554-197X Content not peer-reviewed by ChemRxiv. **License:** CC BY-NC 4.0

$$Rate = k[\mathrm{EC}][^1\mathrm{O}_2], \tag{6}$$

where $[X]$ denotes the concentration of species X and k is the rate coefficient of the reaction, determined using the Eyring equation,

$$k = \frac{k_B T}{h} exp[\frac{-\Delta G^{\ddagger}}{k_B T}], \tag{7}$$

we predict that the initial rate for this reaction would be $Rate_0 = 3.12 \times 10^{-25}$ Ms^{-1}, which is vanishingly small.

We note that previous studies have suggested that EC chemical oxidation does not end with the elimination of a single H_2O molecule. Following this initial chemical oxidation, Jung et al. suggested that further oxidation by $^1O_2$ could result in the evolution of CO_2 and CO,[24] while Rinkel et al. proposed an alternative pathway to CO_2 and glycolic acid.[10] However, given that even the first step of the reaction between EC and $^1O_2$ is highly unlikely to occur, we have chosen not to pursue these downstream reaction pathways.

Compared to the H_2O-forming pathway, the H_2O_2-forming pathway is more straightforward. In a single, concerted step, $^1O_2$ abstracts two hydrogen atoms from the ethylene carbons in EC ($M_1 \longrightarrow M_6$, $\Delta G^{\ddagger} = 1.84$ eV), yielding H_2O_2 and vinylene carbonate (VC). This mechanism is also thermodynamically favorable, with $\Delta G = -0.73$ eV, but due to the high barrier, we do not expect it to occur appreciably at room temperature ($Rate_0 = 1.15 \times 10^{-20}$ Ms^{-1}). We note that previous computational studies have indicated that the reaction EC + $^1O_2 \longrightarrow H_2O_2$ + VC is kinetically limited. Using the complete active space second-order perturbation theory (CASPT2) multireference method with ANO-L-VDZP basis set in vacuum with zero-point energy obtained from DFT, Freiberg et al.[38] predicted a reaction energy barrier $\Delta E^{\ddagger} = 1.27$ eV. Although we cannot directly compare our predictions with these values, as we performed our calculations in an implicit solvent medium and included enthalpic and entropic terms to calculate a free energy barrier, we can

https://doi.org/10.26434/chemrxiv-2023-qr36w **ORCID:** https://orcid.org/0000-0003-1554-197X Content not peer-reviewed by ChemRxiv. **License:** CC BY-NC 4.0

nonetheless say that our prediction agrees qualitatively with the result of Freiberg et al. in that they are significantly larger than what would be expected for a fast reaction.

We have not exhaustively considered all possible reactions between EC and $^1O_2$, but these findings suggest that $^1O_2$ may not be as reactive in the presence of EC as had previously been believed. While potentially surprising, the notion that reactions between EC and $^1O_2$ are slow and therefore kinetically limited appear to be consistent with the most direct evidence of such reactions. Freiberg et al.[38] fully saturated a solution of EC with O_2 and illuminated Rose Bengal, a salt that can photochemically excite $^3O_2$ to $^1O_2$, continuously for one hour to generate $^1O_2$ to react with EC. Using online electrochemical mass spectroscopy, they observed that some O_2 was consumed during the illumination of Rose Bengal, on the order of tens of nanomoles for a mL sample of EC. They also observed the formation of H_2O_2 through colorimetry. Notably, the experiments of Freiberg et al. were performed at 45 C, which should accelerate the reactions between EC and the photogenerated $^1O_2$; in spite of this, the reaction appears to be slow.

More recently, Rinkel et al. performed similar experiments using O_2-saturated EC solutions and Rose Bengal that were designed to promote chemical oxidation of EC.[27] After two hours of illumination, relatively little reactivity between EC and $^1O_2$ was observed. Using solution-phase nuclear magnetic resonance (NMR) spectroscopy, the authors found that the amount of water in the solution increased by roughly a factor of 3, which indicates some reactions took place in the saturated solution. However, the authors began with an electrolyte with water content < 10 ppm, which means that the absolute quantity of water formed was minimal. Moreover, Rinkel et al. were unable to detect other expected reaction products, such as vinylene carbonate (VC) and hydrogen peroxide (H_2O_2), though as Freiberg et al. note,[38] even if VC formed, it may be difficult to detect by NMR due to its low concentration and relative instability.

https://doi.org/10.26434/chemrxiv-2023-qr36w **ORCID:** https://orcid.org/0000-0003-1554-197X Content not peer-reviewed by ChemRxiv. **License:** CC BY-NC 4.0

An Alternate Mechanism for EC Degradation

Our calculations call into question the electrochemical as well as chemical oxidation of EC at LIB positive electrodes. We therefore consider it likely that alternative mechanisms are responsible for the observed reactivity of EC at elevated potentials.

We propose one such alternative: that EC may indeed combine with "reactive oxygen", but that the "reactive oxygen" is comprised of *oxygen anions* superoxide (O_2^{-1}) and/or peroxide (O_2^{-2}), rather than $^1O_2$. This explanation is consistent with the existing literature on oxygen in LIB positive electrodes. It is well known that oxygen redox occurs within many oxide positive electrodes during battery charging and discharging.[39–43] Both experimental and theoretical studies have observed peroxides or "peroxo-like" oxygen dimers in the electrode bulk.[44–46] These dimers have been suggested as intermediates that can eventually lead to neutral O_2 evolution. More recently, Genreith-Schriever et al.[47] performed *ab initio* molecular dynamics simulations on $LiNiO_2$ electrodes and showed that peroxide dimers form on the electrode surface, which is more directly related to oxygen loss and reactions with electrolyte molecules. Moreover, superoxide species are believed to be important intermediates in metal-air batteries, where they have been linked to the decomposition of carbonate solvents.[48–50]

As with $^1O_2$, we identified a number of elementary reaction mechanisms between EC and either O_2^{-1} (Figure 3) or O_2^{-2} (Figure 4) using DFT. It is worth noting that these mechanisms are only suggestions of the initial steps of EC decomposition, and further work must be done to examine how these reactions may lead to more stable decomposition products.

We find that O_2^{-1} cannot abstract protons or hydrogen atoms from EC to form H_2O_2. The first hydrogen abstraction ($M_7 \longrightarrow M_8$) suffers from a high free energy barrier ($\Delta G^\ddagger = 1.70$ eV) and is thermodynamically unfavorable ($\Delta G = 1.62$ eV). The removal of an additional proton to form H_2O_2 and reduced radical VC is also somewhat unfavorable ($M_8 \longrightarrow M_9$; $\Delta G = 0.08$ eV) but has a modest barrier of $\Delta G^\ddagger = 0.11$ eV.

While O_2^{-1} may not be able to attack EC's protons, it can attack the ethylene carbons, in

https://doi.org/10.26434/chemrxiv-2023-qr36w **ORCID:** https://orcid.org/0000-0003-1554-197X Content not peer-reviewed by ChemRxiv. **License:** CC BY-NC 4.0

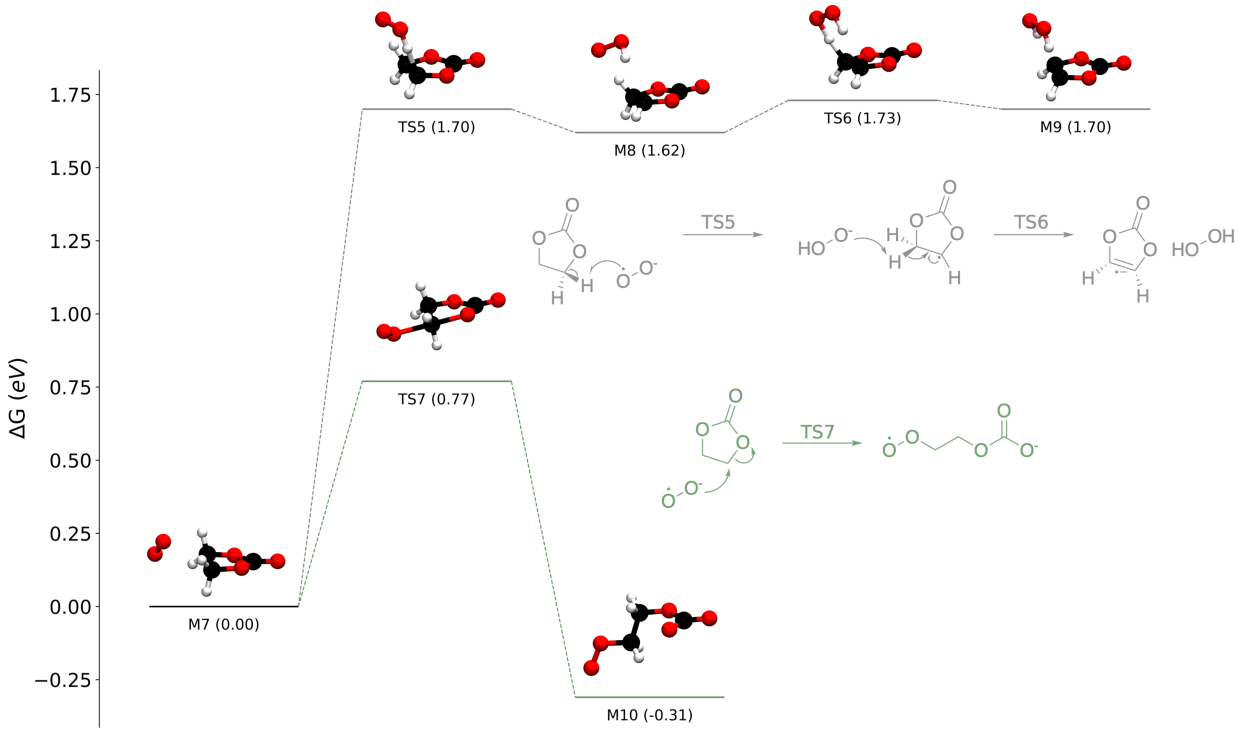

Figure 3: Energy diagrams for reactions between EC and superoxide (O_2^{-1}), including a route forming H_2O_2 and reduced VC (gray) and a nucleophilic substitution (green).

agreement with previous studies focused on Li−O_2 batteries.[51] We identified a nucleophilic substitution reaction $M_7 \longrightarrow M_{10}$. This reaction is favorable ($\Delta G = -0.31$ eV), and while it is not predicted to be rapid ($\Delta G^{\ddagger} = 0.77$ eV), it is considerably faster than any $^1O_2$ reaction that we have identified. For comparison, if we consider the same conditions as we did previously (O_2^{-1} at the saturation concentration of O_2 dissolved in pure EC at room temperature), the initial rate for $M_7 \longrightarrow M_{10}$ is predicted to be $Rate_0 = 0.014$ Ms^{-1} — more than 20 orders of magnitude faster than $M_1 \longrightarrow M_2$. Aside from the predicted energy barrier, the reaction $M_7 \longrightarrow M_{10}$ appears plausible based on previous experimental observations. Specifically, Kaufman and McCloskey recently used differential electrochemical mass spectroscopy to observe electrolyte decomposition products that formed at lithium-excess NMC electrodes;[21] they observed peroxide-containing products similar to M_{10} and even hypothesized that such species could form via nucleophilic substitution.

Reactions with peroxide are even more facile. Whereas proton abstraction is unfavorable

https://doi.org/10.26434/chemrxiv-2023-qr36w **ORCID:** https://orcid.org/0000-0003-1554-197X Content not peer-reviewed by ChemRxiv. **License:** CC BY-NC 4.0

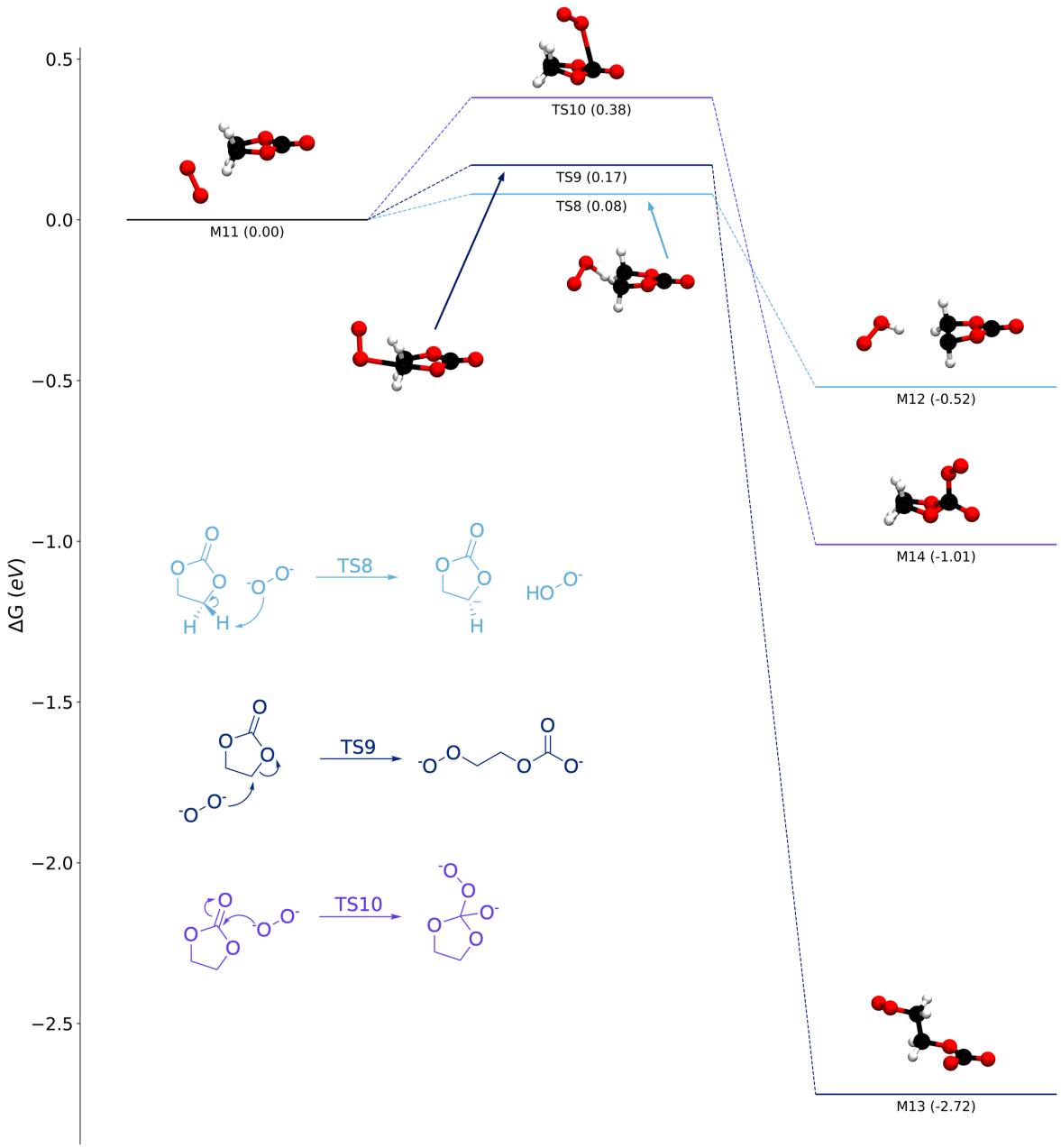

Figure 4: Energy diagrams for reactions between EC and peroxide ($O_2{}^{-2}$): proton abstraction (light blue), nucleophilic substitution (dark blue), and addition to form a tetrahedral complex (purple).

for superoxide, it is predicted to occur rapidly for peroxide ($M_{11} \longrightarrow M_{12}$; $\Delta G^{\ddagger} = 0.08$ eV). Similarly, nucleophilic attack on the ethylene carbons of EC by $O_2{}^{-2}$ is extremely favorable and rapid ($M_{11} \longrightarrow M_{13}$; $\Delta G = -2.72$ eV; $\Delta G^{\ddagger} = 0.17$ eV). Finally, we predict that peroxide can attach to the carbonate carbon of EC, forming a tetrahedral complex ($M_{11} \longrightarrow$

https://doi.org/10.26434/chemrxiv-2023-qr36w **ORCID:** https://orcid.org/0000-0003-1554-197X Content not peer-reviewed by ChemRxiv. **License:** CC BY-NC 4.0

M_{14}; $\Delta G^{\ddagger} = 0.38$ eV).

https://doi.org/10.26434/chemrxiv-2023-qr36w **ORCID:** https://orcid.org/0000-0003-1554-197X Content not peer-reviewed by ChemRxiv. **License:** CC BY-NC 4.0

Conclusions and Future Work

Here, we have used first-principles DFT calculations to examine common explanations for high-potential electrolyte degradation in LIBs, focusing on model EC-based electrolytes. Even after accounting for the effect of concentration, we found that purely electrochemical oxidation of EC is thermodynamically disfavored at essentially any potential relevant to normal LIB operation. We likewise cast doubt on hypotheses related to $^1O_2$, as both of the major reactions reported in the literature are predicted to have large kinetic barriers, making them extremely sluggish under ambient conditions.

Based on previous studies of oxygen redox in LIB positive electrodes, we suggest the possibility that EC may react with oxygen anions instead of neutral $^1O_2$. These anionic species are likely to be formed on transition metal oxide surfaces as an intermediate prior to neutral O_2 release. Our initial calculations show that EC can react rapidly with ${O_2}^{-1}$ and especially ${O_2}^{-2}$. Additional studies, both computational and experimental, should now be undertaken to assess i) how easily these anion species can form on NMC, DRX, or other oxide electrode surfaces; ii) the lifetime of these anions; and iii) if they can be eliminated from the electrode surface to react homogeneously with the electrolyte, as we have assumed here. We emphasize that, in the present work, we have considered only the initial reactions between EC and oxygen anions. Even if these reactions do occur, we do not yet know if these reactions can lead to observed products, such as water and acids, nor what other products and intermediates may be formed. In the future, we intend to use CRN-based methods to more thoroughly explore reactions between EC and oxygen anions.

In this study, we have largely ignored the role of electrode surfaces, treating the electrode mainly as a sink for electrons or as a source of various "reactive oxygen" species. However, electrode active material may also directly participate in reactions with electrolyte components like EC or may act as catalysts. For instance, it has been suggested that EC dehydrogenates on transition metal oxides.[27,34,52] While some initial studies of electrolyte reactions with oxide positive electrodes have been conducted using DFT,[53–55] they have

https://doi.org/10.26434/chemrxiv-2023-qr36w **ORCID:** https://orcid.org/0000-0003-1554-197X Content not peer-reviewed by ChemRxiv. **License:** CC BY-NC 4.0

typically been limited to examining a small number of reactions or performing very short dynamic simulations on the order of picoseconds. We hope that further computational studies consider the possible reactive and catalytic nature of LIB positive electrodes in more detail.

Finally, for purposes of simplicity and computational cost, we have mostly neglected the role of explicit solvation shells in this work. As strong solvent effects have been identified for particular electrolyte decomposition reactions,[56] we cannot discount the possibility that the reaction kinetics reported here may be affected by the presence of explicit solvent molecules. Calculations involving complete solvent clusters should be performed to determine if explicit solvation affects reactions between EC and $^1O_2$, O_2^{-1}, or O_2^{-2}.

https://doi.org/10.26434/chemrxiv-2023-qr36w **ORCID:** https://orcid.org/0000-0003-1554-197X Content not peer-reviewed by ChemRxiv. **License:** CC BY-NC 4.0

Conflicts of interest

There are no conflicts to declare.

Supporting Information

Software availability; data availability; computational methods. Cited references:[57–67]

Acknowledgements

E.W.C.S.-S. was supported by the Kavli Energy NanoScience Institute Philomathia Graduate Student Fellowship. S.V. was supported by the Betty and Gordon Moore Foundation. T.B.P. conducted this work as part of the Community College Internship program under the U.S. Department of Energy, Office of Science, Office of Workforce Development for Teachers and Scientists. Additional support comes from the Silicon Consortium Project (SCP) directed by Brian Cunningham under the Assistant Secretary for Energy Efficiency and Renewable Energy, Office of Vehicle Technologies of the U.S. Department of Energy, Contract No. DE-AC02-05CH11231, as well as the Disordered Rock Salt Consortium (DRX+) program directed by Tien Duong under the Assistant Secretary for Energy Efficiency and Renewable Energy, Office of Vehicle Technologies of the U.S. Department of Energy, Contract No. DE-AC02-05CH11231. The authors thank M. Rohith Srinivaas for useful discussions.

Author Contributions

- E.W.C.S.-S.: Conceptualization; formal analysis; funding acquisition; investigation; methodology; supervision; visualization; writing — original draft; writing — review & editing
- S.V.: Conceptualization; formal analysis; investigation; methodology; visualization;

https://doi.org/10.26434/chemrxiv-2023-qr36w **ORCID:** https://orcid.org/0000-0003-1554-197X Content not peer-reviewed by ChemRxiv. **License:** CC BY-NC 4.0

writing — original draft; writing — review & editing

- T.B.P.: Investigation
- B.L.D.R.: Conceptualization; writing — review & editing
- B.D.M.: Funding acquisition; supervision
- K.A.P.: Funding acquisition; resources; supervision; writing — review & editing

https://doi.org/10.26434/chemrxiv-2023-qr36w **ORCID:** https://orcid.org/0000-0003-1554-197X Content not peer-reviewed by ChemRxiv. **License:** CC BY-NC 4.0

References

(1) Xu, K. Nonaqueous Liquid Electrolytes for Lithium-Based Rechargeable Batteries. *Chemical Reviews* **2004**, *104*, 4303–4418.

(2) Heiskanen, S. K.; Laszczynski, N.; Lucht, B. L. Perspective—surface reactions of electrolyte with LiNixCoyMnzO2 cathodes for lithium ion batteries. *Journal of the Electrochemical Society* **2020**, *167*, 100519.

(3) Wang, M.; Chen, X.; Yao, H.; Lin, G.; Lee, J.; Chen, Y.; Chen, Q. Research Progress in Lithium-Excess Disordered Rock-Salt Oxides Cathode. *Energy & Environmental Materials* **2022**, *5*, 1139–1154.

(4) Xu, K. Electrolytes and Interphases in Li-Ion Batteries and Beyond. *Chemical Reviews* **2014**, *114*, 11503–11618.

(5) Winter, M. The Solid Electrolyte Interphase – The Most Important and the Least Understood Solid Electrolyte in Rechargeable Li Batteries. *Zeitschrift für Physikalische Chemie* **2009**, *223*, 1395–1406.

(6) Kühn, S. P.; Edström, K.; Winter, M.; Cekic-Laskovic, I. Face to Face at the Cathode Electrolyte Interphase: From Interface Features to Interphase Formation and Dynamics. *Advanced Materials Interfaces* **2022**, *9*, 2102078.

(7) Blomgren, G. E. Electrolytes for advanced batteries. *Journal of Power Sources* **1999**, *81-82*, 112–118.

(8) Zhang, S. S.; Jow, T. R.; Amine, K.; Henriksen, G. L. LiPF6–EC–EMC electrolyte for Li-ion battery. *Journal of Power Sources* **2002**, *107*, 18–23.

(9) Nie, M.; Chalasani, D.; Abraham, D. P.; Chen, Y.; Bose, A.; Lucht, B. L. Lithium Ion Battery Graphite Solid Electrolyte Interphase Revealed by Microscopy and Spectroscopy. *The Journal of Physical Chemistry C* **2013**, *117*, 1257–1267.

https://doi.org/10.26434/chemrxiv-2023-qr36w **ORCID:** https://orcid.org/0000-0003-1554-197X Content not peer-reviewed by ChemRxiv. **License:** CC BY-NC 4.0

(10) Rinkel, B. L. D.; Hall, D. S.; Temprano, I.; Grey, C. P. Electrolyte Oxidation Pathways in Lithium-Ion Batteries. *Journal of the American Chemical Society* **2020**, *142*, 15058–15074.

(11) Wang, Y.; Nakamura, S.; Ue, M.; Balbuena, P. B. Theoretical Studies To Understand Surface Chemistry on Carbon Anodes for Lithium-Ion Batteries: Reduction Mechanisms of Ethylene Carbonate. *Journal of the American Chemical Society* **2001**, *123*, 11708–11718.

(12) Kuai, D.; Balbuena, P. B. Solvent Degradation and Polymerization in the Li-Metal Battery: Organic-Phase Formation in Solid-Electrolyte Interphases. *ACS Applied Materials & Interfaces* **2022**, *14*, 2817–2824.

(13) Spotte-Smith, E. W. C.; Petrocelli, T. B.; Patel, H. D.; Blau, S. M.; Persson, K. A. Elementary Decomposition Mechanisms of Lithium Hexafluorophosphate in Battery Electrolytes and Interphases. *ACS Energy Letters* **2023**, *8*, 347–355.

(14) Barter, D.; Spotte-Smith, E. W. C.; S. Redkar, N.; Khanwale, A.; Dwaraknath, S.; A. Persson, K.; M. Blau, S. Predictive stochastic analysis of massive filter-based electrochemical reaction networks. *Digital Discovery* **2023**, *2*, 123–137.

(15) Spotte-Smith, E. W. C.; Kam, R. L.; Barter, D.; Xie, X.; Hou, T.; Dwaraknath, S.; Blau, S. M.; Persson, K. A. Toward a Mechanistic Model of Solid–Electrolyte Interphase Formation and Evolution in Lithium-Ion Batteries. *ACS Energy Letters* **2022**, *7*, 1446–1453.

(16) Azcarate, I.; Yin, W.; Méthivier, C.; Ribot, F.; Laberty-Robert, C.; Grimaud, A. Assessing the Oxidation Behavior of EC:DMC Based Electrolyte on Non-Catalytically Active Surface. *Journal of The Electrochemical Society* **2020**, *167*, 080530.

(17) Rowden, B.; Garcia-Araez, N. A review of gas evolution in lithium ion batteries. *Energy Reports* **2020**, *6*, 10–18.

https://doi.org/10.26434/chemrxiv-2023-qr36w **ORCID:** https://orcid.org/0000-0003-1554-197X Content not peer-reviewed by ChemRxiv. **License:** CC BY-NC 4.0

(18) Dose, W. M.; Li, W.; Temprano, I.; O'Keefe, C. A.; Mehdi, B. L.; De Volder, M. F.; Grey, C. P. Onset potential for electrolyte oxidation and Ni-rich cathode degradation in lithium-ion batteries. *ACS Energy Letters* **2022**, *7*, 3524–3530.

(19) Xing, L.; Borodin, O. Oxidation induced decomposition of ethylene carbonate from DFT calculations – importance of explicitly treating surrounding solvent. *Physical Chemistry Chemical Physics* **2012**, *14*, 12838–12843.

(20) Fell, C. R.; Qian, D.; Carroll, K. J.; Chi, M.; Jones, J. L.; Meng, Y. S. Correlation Between Oxygen Vacancy, Microstrain, and Cation Distribution in Lithium-Excess Layered Oxides During the First Electrochemical Cycle. *Chemistry of Materials* **2013**, *25*, 1621–1629.

(21) Kaufman, L. A.; McCloskey, B. D. Surface Lithium Carbonate Influences Electrolyte Degradation via Reactive Oxygen Attack in Lithium-Excess Cathode Materials. *Chemistry of Materials* **2021**, *33*, 4170–4176.

(22) Luo, K.; Roberts, M. R.; Hao, R.; Guerrini, N.; Pickup, D. M.; Liu, Y.-S.; Edström, K.; Guo, J.; Chadwick, A. V.; Duda, L. C.; Bruce, P. G. Charge-compensation in 3d-transition-metal-oxide intercalation cathodes through the generation of localized electron holes on oxygen. *Nature Chemistry* **2016**, *8*, 684–691.

(23) Lun, Z.; Ouyang, B.; Kitchaev, D. A.; Clément, R. J.; Papp, J. K.; Balasubramanian, M.; Tian, Y.; Lei, T.; Shi, T.; McCloskey, B. D.; Lee, J.; Ceder, G. Improved Cycling Performance of Li-Excess Cation-Disordered Cathode Materials upon Fluorine Substitution. *Advanced Energy Materials* **2019**, *9*, 1802959.

(24) Jung, R.; Metzger, M.; Maglia, F.; Stinner, C.; Gasteiger, H. A. Oxygen Release and Its Effect on the Cycling Stability of LiNixMnyCozO2 (NMC) Cathode Materials for Li-Ion Batteries. *Journal of The Electrochemical Society* **2017**, *164*, A1361.

https://doi.org/10.26434/chemrxiv-2023-qr36w **ORCID:** https://orcid.org/0000-0003-1554-197X Content not peer-reviewed by ChemRxiv. **License:** CC BY-NC 4.0

(25) Jung, R.; Metzger, M.; Maglia, F.; Stinner, C.; Gasteiger, H. A. Chemical versus Electrochemical Electrolyte Oxidation on NMC111, NMC622, NMC811, LNMO, and Conductive Carbon. *The Journal of Physical Chemistry Letters* **2017**, *8*, 4820–4825.

(26) Wandt, J.; Freiberg, A. T.; Ogrodnik, A.; Gasteiger, H. A. Singlet oxygen evolution from layered transition metal oxide cathode materials and its implications for lithium-ion batteries. *Materials Today* **2018**, *21*, 825–833.

(27) Rinkel, B. L. D.; Vivek, J. P.; Garcia-Araez, N.; Grey, C. P. Two electrolyte decomposition pathways at nickel-rich cathode surfaces in lithium-ion batteries. *Energy & Environmental Science* **2022**, *15*, 3416–3438.

(28) Clennan, E. L. New mechanistic and synthetic aspects of singlet oxygen chemistry. *Tetrahedron* **2000**, *56*, 9151–9179.

(29) Al-Nu'airat, J.; Oluwoye, I.; Zeinali, N.; Altarawneh, M.; Dlugogorski, B. Z. Review of chemical reactivity of singlet oxygen with organic fuels and contaminants. *The Chemical Record* **2021**, *21*, 315–342.

(30) Ue, M.; Takeda, M.; Takehara, M.; Mori, S. Electrochemical Properties of Quaternary Ammonium Salts for Electrochemical Capacitors. *Journal of The Electrochemical Society* **1997**, *144*, 2684.

(31) Xu, K.; Ding, S. P.; Jow, T. R. Toward Reliable Values of Electrochemical Stability Limits for Electrolytes. *Journal of The Electrochemical Society* **1999**, *146*, 4172–4178.

(32) Abe, K.; Ushigoe, Y.; Yoshitake, H.; Yoshio, M. Functional electrolytes: Novel type additives for cathode materials, providing high cycleability performance. *Journal of Power Sources* **2006**, *153*, 328–335.

(33) Metzger, M.; Marino, C.; Sicklinger, J.; Haering, D.; Gasteiger, H. A. Anodic Oxidation of Conductive Carbon and Ethylene Carbonate in High-Voltage Li-Ion Batteries Quan-

https://doi.org/10.26434/chemrxiv-2023-qr36w **ORCID:** https://orcid.org/0000-0003-1554-197X Content not peer-reviewed by ChemRxiv. **License:** CC BY-NC 4.0

tified by On-Line Electrochemical Mass Spectrometry. *Journal of The Electrochemical Society* **2015**, *162*, A1123–A1134.

(34) Zhang, Y.; Katayama, Y.; Tatara, R.; Giordano, L.; Yu, Y.; Fraggedakis, D.; Sun, J. G.; Maglia, F.; Jung, R.; Bazant, M. Z.; Shao-Horn, Y. Revealing electrolyte oxidation via carbonate dehydrogenation on Ni-based oxides in Li-ion batteries by in situ Fourier transform infrared spectroscopy. *Energy & Environmental Science* **2020**, *13*, 183–199.

(35) Chen, Z. Chasing protons in lithium-ion batteries. *Chemical Communications* **2022**, *58*, 10127–10135.

(36) Maletin, Y. A.; Cannon, R. D. Dissociative electron transfer reactions. *Theoretical and experimental chemistry* **1998**, *34*, 57–68.

(37) Trasatti, S. The absolute electrode potential: an explanatory note (Recommendations 1986). *Pure and Applied Chemistry* **1986**, *58*, 955–966.

(38) Freiberg, A. T. S.; Roos, M. K.; Wandt, J.; De Vivie-Riedle, R.; Gasteiger, H. A. Singlet Oxygen Reactivity with Carbonate Solvents Used for Li-Ion Battery Electrolytes. *The Journal of Physical Chemistry A* **2018**, *122*, 8828–8839.

(39) Tarascon, J.; Vaughan, G.; Chabre, Y.; Seguin, L.; Anne, M.; Strobel, P.; Amatucci, G. In situ structural and electrochemical study of Ni1- xCoxO2 metastable oxides prepared by soft chemistry. *Journal of solid state chemistry* **1999**, *147*, 410–420.

(40) Lee, E.; Persson, K. A. Structural and chemical evolution of the layered Li-excess LixMnO3 as a function of Li content from first-principles calculations. *Advanced Energy Materials* **2014**, *4*, 1400498.

(41) Wang, R.; Li, X.; Liu, L.; Lee, J.; Seo, D.-H.; Bo, S.-H.; Urban, A.; Ceder, G. A disordered rock-salt Li-excess cathode material with high capacity and substantial oxy-

https://doi.org/10.26434/chemrxiv-2023-qr36w **ORCID:** https://orcid.org/0000-0003-1554-197X Content not peer-reviewed by ChemRxiv. **License:** CC BY-NC 4.0

gen redox activity: Li1.25Nb0.25Mn0.5O2. *Electrochemistry Communications* **2015**, *60*, 70–73.

(42) Grenier, A.; Kamm, G. E.; Li, Y.; Chung, H.; Meng, Y. S.; Chapman, K. W. Nanostructure Transformation as a Signature of Oxygen Redox in Li-Rich 3d and 4d Cathodes. *Journal of the American Chemical Society* **2021**, *143*, 5763–5770.

(43) Huang, T.-Y.; Cai, Z.; Crafton, M. J.; Kaufman, L. A.; Konz, Z. M.; Bergstrom, H. K.; Kedzie, E. A.; Hao, H.-M.; Ceder, G.; McCloskey, B. D. Quantitative Decoupling of Oxygen-Redox and Manganese-Redox Voltage Hysteresis in a Cation-Disordered Rock Salt Cathode. *Advanced Energy Materials* **2023**, *13*, 2300241.

(44) McCalla, E.; Abakumov, A. M.; Saubanère, M.; Foix, D.; Berg, E. J.; Rousse, G.; Doublet, M.-L.; Gonbeau, D.; Novák, P.; Van Tendeloo, G.; Dominko, R.; Tarascon, J.-M. Visualization of O-O peroxo-like dimers in high-capacity layered oxides for Li-ion batteries. *Science* **2015**, *350*, 1516–1521.

(45) Saubanère, M.; McCalla, E.; Tarascon, J.-M.; Doublet, M.-L. The intriguing question of anionic redox in high-energy density cathodes for Li-ion batteries. *Energy & Environmental Science* **2016**, *9*, 984–991.

(46) Hong, J.; Gent, W. E.; Xiao, P.; Lim, K.; Seo, D.-H.; Wu, J.; Csernica, P. M.; Takacs, C. J.; Nordlund, D.; Sun, C.-J.; Stone, K. H.; Passarello, D.; Yang, W.; Prendergast, D.; Ceder, G.; Toney, M. F.; Chueh, W. C. Metal–oxygen decoordination stabilizes anion redox in Li-rich oxides. *Nature Materials* **2019**, *18*, 256–265.

(47) Genreith-Schriever, A. R.; Banerjee, H.; Menon, A. S.; Bassey, E. N.; Piper, L. F.; Grey, C. P.; Morris, A. J. Oxygen hole formation controls stability in LiNiO2 cathodes. *Joule* **2023**, *7*, 1623–1640.

(48) Yang, J.; Zhai, D.; Wang, H.-H.; Lau, K. C.; Schlueter, J. A.; Du, P.; Myers, D. J.; Sun, Y.-K.; Curtiss, L. A.; Amine, K. Evidence for lithium superoxide-like species in

https://doi.org/10.26434/chemrxiv-2023-qr36w **ORCID:** https://orcid.org/0000-0003-1554-197X Content not peer-reviewed by ChemRxiv. **License:** CC BY-NC 4.0

the discharge product of a Li–O2 battery. *Physical Chemistry Chemical Physics* **2013**, *15*, 3764–3771.

(49) Zhai, D.; Wang, H.-H.; Lau, K. C.; Gao, J.; Redfern, P. C.; Kang, F.; Li, B.; Indacochea, E.; Das, U.; Sun, H.-H.; Sun, H.-J.; Amine, K.; Curtiss, L. A. Raman Evidence for Late Stage Disproportionation in a Li–O2 Battery. *The Journal of Physical Chemistry Letters* **2014**, *5*, 2705–2710.

(50) Wang, Y.; Lu, Y.-R.; Dong, C.-L.; Lu, Y.-C. Critical Factors Controlling Superoxide Reactions in Lithium–Oxygen Batteries. *ACS Energy Letters* **2020**, *5*, 1355–1363.

(51) Bryantsev, V. S.; Giordani, V.; Walker, W.; Blanco, M.; Zecevic, S.; Sasaki, K.; Uddin, J.; Addison, D.; Chase, G. V. Predicting Solvent Stability in Aprotic Electrolyte Li–Air Batteries: Nucleophilic Substitution by the Superoxide Anion Radical ($O_2^{\bullet-}$). *The Journal of Physical Chemistry A* **2011**, *115*, 12399–12409.

(52) Giordano, L.; Karayaylali, P.; Yu, Y.; Katayama, Y.; Maglia, F.; Lux, S.; Shao-Horn, Y. Chemical reactivity descriptor for the oxide-electrolyte interface in Li-ion batteries. *The journal of physical chemistry letters* **2017**, *8*, 3881–3887.

(53) Kumar, N.; Leung, K.; Siegel, D. J. Crystal Surface and State of Charge Dependencies of Electrolyte Decomposition on LiMn2O4 Cathode. *Journal of The Electrochemical Society* **2014**, *161*, E3059.

(54) Choi, D.; Kang, J.; Park, J.; Han, B. First-principles study on thermodynamic stability of the hybrid interfacial structure of LiMn 2 O 4 cathode and carbonate electrolyte in Li-ion batteries. *Physical Chemistry Chemical Physics* **2018**, *20*, 11592–11597.

(55) Xu, S.; Luo, G.; Jacobs, R.; Fang, S.; Mahanthappa, M. K.; Hamers, R. J.; Morgan, D. Ab Initio Modeling of Electrolyte Molecule Ethylene Carbonate Decomposition Reaction on Li(Ni,Mn,Co)O_2 Cathode Surface. *ACS Applied Materials & Interfaces* **2017**, *9*, 20545–20553.

https://doi.org/10.26434/chemrxiv-2023-qr36w **ORCID:** https://orcid.org/0000-0003-1554-197X Content not peer-reviewed by ChemRxiv. **License:** CC BY-NC 4.0

(56) Boyer, M. J.; Hwang, G. S. Theoretical Prediction of the Strong Solvent Effect on Reduced Ethylene Carbonate Ring-Opening and Its Impact on Solid Electrolyte Interphase Evolution. *The Journal of Physical Chemistry C* **2019**, *123*, 17695–17702.

(57) Spotte-Smith, E. W. C.; Vijay, S.; Petrocelli, T. B.; Rinkel, B. L. D.; McCloskey, B. D.; Persson, K. A. Data for "". 2023; DOI:10.6084/m9.figshare.24589056.

(58) Ong, S. P.; Richards, W. D.; Jain, A.; Hautier, G.; Kocher, M.; Cholia, S.; Gunter, D.; Chevrier, V. L.; Persson, K. A.; Ceder, G. Python Materials Genomics (pymatgen): A robust, open-source python library for materials analysis. *Computational Materials Science* **2013**, *68*, 314–319.

(59) Epifanovsky, E.; Gilbert, A. T. B.; Feng, X.; Lee, J.; Mao, Y.; Mardirossian, N.; Pokhilko, P.; White, A. F.; Coons, M. P.; Dempwolff, A. L.; Gan, Z.; Hait, D.; Horn, P. R.; Jacobson, L. D.; Kaliman, I.; Kussmann, J.; Lange, A. W.; Lao, K. U.; Levine, D. S.; Liu, J.; McKenzie, S. C.; Morrison, A. F.; Nanda, K. D.; Plasser, F.; Rehn, D. R.; Vidal, M. L.; You, Z.-Q.; Zhu, Y.; Alam, B.; Albrecht, B. J.; Aldossary, A.; Alguire, E.; Andersen, J. H.; Athavale, V.; Barton, D.; Begam, K.; Behn, A.; Bellonzi, N.; Bernard, Y. A.; Berquist, E. J.; Burton, H. G. A.; Carreras, A.; Carter-Fenk, K.; Chakraborty, R.; Chien, A. D.; Closser, K. D.; Cofer-Shabica, V.; Dasgupta, S.; de Wergifosse, M.; Deng, J.; Diedenhofen, M.; Do, H.; Ehlert, S.; Fang, P.-T.; Fatehi, S.; Feng, Q.; Friedhoff, T.; Gayvert, J.; Ge, Q.; Gidofalvi, G.; Goldey, M.; Gomes, J.; González-Espinoza, C. E.; Gulania, S.; Gunina, A. O.; Hanson-Heine, M. W. D.; Harbach, P. H. P.; Hauser, A.; Herbst, M. F.; Hernández Vera, M.; Hodecker, M.; Holden, Z. C.; Houck, S.; Huang, X.; Hui, K.; Huynh, B. C.; Ivanov, M.; Jász, ; Ji, H.; Jiang, H.; Kaduk, B.; Kähler, S.; Khistyaev, K.; Kim, J.; Kis, G.; Klunzinger, P.; Koczor-Benda, Z.; Koh, J. H.; Kosenkov, D.; Koulias, L.; Kowalczyk, T.; Krauter, C. M.; Kue, K.; Kunitsa, A.; Kus, T.; Ladjánszki, I.; Landau, A.; Lawler, K. V.; Lefrancois, D.; Lehtola, S.; Li, R. R.; Li, Y.-P.; Liang, J.; Lieben-

https://doi.org/10.26434/chemrxiv-2023-qr36w **ORCID:** https://orcid.org/0000-0003-1554-197X Content not peer-reviewed by ChemRxiv. **License:** CC BY-NC 4.0

thal, M.; Lin, H.-H.; Lin, Y.-S.; Liu, F.; Liu, K.-Y.; Loipersberger, M.; Luenser, A.; Manjanath, A.; Manohar, P.; Mansoor, E.; Manzer, S. F.; Mao, S.-P.; Marenich, A. V.; Markovich, T.; Mason, S.; Maurer, S. A.; McLaughlin, P. F.; Menger, M. F. S. J.; Mewes, J.-M.; Mewes, S. A.; Morgante, P.; Mullinax, J. W.; Oosterbaan, K. J.; Paran, G.; Paul, A. C.; Paul, S. K.; Pavošević, F.; Pei, Z.; Prager, S.; Proynov, E. I.; Rák, ; Ramos-Cordoba, E.; Rana, B.; Rask, A. E.; Rettig, A.; Richard, R. M.; Rob, F.; Rossomme, E.; Scheele, T.; Scheurer, M.; Schneider, M.; Sergueev, N.; Sharada, S. M.; Skomorowski, W.; Small, D. W.; Stein, C. J.; Su, Y.-C.; Sundstrom, E. J.; Tao, Z.; Thirman, J.; Tornai, G. J.; Tsuchimochi, T.; Tubman, N. M.; Veccham, S. P.; Vydrov, O.; Wenzel, J.; Witte, J.; Yamada, A.; Yao, K.; Yeganeh, S.; Yost, S. R.; Zech, A.; Zhang, I. Y.; Zhang, X.; Zhang, Y.; Zuev, D.; Aspuru-Guzik, A.; Bell, A. T.; Besley, N. A.; Bravaya, K. B.; Brooks, B. R.; Casanova, D.; Chai, J.-D.; Coriani, S.; Cramer, C. J.; Cserey, G.; DePrince, A. E., III; DiStasio, R. A., Jr.; Dreuw, A.; Dunietz, B. D.; Furlani, T. R.; Goddard, W. A., III; Hammes-Schiffer, S.; Head-Gordon, T.; Hehre, W. J.; Hsu, C.-P.; Jagau, T.-C.; Jung, Y.; Klamt, A.; Kong, J.; Lambrecht, D. S.; Liang, W.; Mayhall, N. J.; McCurdy, C. W.; Neaton, J. B.; Ochsenfeld, C.; Parkhill, J. A.; Peverati, R.; Rassolov, V. A.; Shao, Y.; Slipchenko, L. V.; Stauch, T.; Steele, R. P.; Subotnik, J. E.; Thom, A. J. W.; Tkatchenko, A.; Truhlar, D. G.; Van Voorhis, T.; Wesolowski, T. A.; Whaley, K. B.; Woodcock, H. L., III; Zimmerman, P. M.; Faraji, S.; Gill, P. M. W.; Head-Gordon, M.; Herbert, J. M.; Krylov, A. I. Software for the frontiers of quantum chemistry: An overview of developments in the Q-Chem 5 package. *The Journal of Chemical Physics* **2021**, *155*, 084801.

(60) Mardirossian, N.; Head-Gordon, M. B97X-V: A 10-parameter, range-separated hybrid, generalized gradient approximation density functional with nonlocal correlation, designed by a survival-of-the-fittest strategy. *Physical Chemistry Chemical Physics* **2014**, *16*, 9904–9924.

https://doi.org/10.26434/chemrxiv-2023-qr36w **ORCID:** https://orcid.org/0000-0003-1554-197X Content not peer-reviewed by ChemRxiv. **License:** CC BY-NC 4.0

(61) Rappoport, D.; Furche, F. Property-optimized Gaussian basis sets for molecular response calculations. *The Journal of Chemical Physics* **2010**, *133*, 134105.

(62) Marenich, A. V.; Cramer, C. J.; Truhlar, D. G. Universal Solvation Model Based on Solute Electron Density and on a Continuum Model of the Solvent Defined by the Bulk Dielectric Constant and Atomic Surface Tensions. *The Journal of Physical Chemistry B* **2009**, *113*, 6378–6396.

(63) Spotte-Smith, E. W. C.; Blau, S. M.; Xie, X.; Patel, H. D.; Wen, M.; Wood, B.; Dwaraknath, S.; Persson, K. A. Quantum chemical calculations of lithium-ion battery electrolyte and interphase species. *Scientific Data* **2021**, *8*, 203.

(64) Mullinax, J. W.; Bauschlicher, C. W. J.; Lawson, J. W. Reaction of Singlet Oxygen with the Ethylene Group: Implications for Electrolyte Stability in Li-Ion and Li-O2 Batteries. *The Journal of Physical Chemistry A* **2021**, *125*, 2876–2884.

(65) Schweitzer, C.; Schmidt, R. Physical Mechanisms of Generation and Deactivation of Singlet Oxygen. *Chemical Reviews* **2003**, *103*, 1685–1758.

(66) Ervin, K. M.; Anusiewicz, I.; Skurski, P.; Simons, J.; Lineberger, W. C. The Only Stable State of O_2^- Is the $X\ ^2\Pi_g$ Ground State and It (Still!) Has an Adiabatic Electron Detachment Energy of 0.45 eV. *The Journal of Physical Chemistry A* **2003**, *107*, 8521–8529.

(67) Read, J.; Mutolo, K.; Ervin, M.; Behl, W.; Wolfenstine, J.; Driedger, A.; Foster, D. Oxygen transport properties of organic electrolytes and performance of lithium/oxygen battery. *Journal of the Electrochemical Society* **2003**, *150*, A1351.

https://doi.org/10.26434/chemrxiv-2023-qr36w **ORCID:** https://orcid.org/0000-0003-1554-197X Content not peer-reviewed by ChemRxiv. **License:** CC BY-NC 4.0